Carbonic acid buffer species measured in real time with an intracellular microelectrode array

Kristina Wietasch and **Richard P. Kraig**

Departments of Neurology and Pharmacological and Physiological Sciences, The University of Chicago, Chicago, Illinois 60637

Abstract

Carbonic acid buffer anions, HCO_3^- and CO_3^{2-}, play an instrumental role in a host of vital processes in animal cells and tissues. Yet study of carbonic acid buffer species is hampered because no means are available to simultaneously monitor them at a cellular level in a rapid and dynamic fashion. An ion-selective cocktail, previously reported to measure changes in bicarbonate activity $(\alpha_{HCO_3^-})$, was instead shown to be principally selective for $\alpha_{CO_3^{2-}}$. Ion-selective micropipettes (ISMs) based on this exchanger and consisting of a 3:1:6 (volume) mixture of tri-*n*-octylpropylammonium chloride, 1-octanol, and trifluoroacetyl-*p*-butylbenzene showed no significant interference from bicarbonate, chloride, phosphate, ascorbate, lactate, glutamate, acetate, or hydroxyl ions at concentrations expected in vivo. Intracellular and triple-barrel ISMs, consisting of a CO_3^{2-}-sensitive, pH-sensitive, and reference barrel, were fabricated. Skeletal muscle cells ($n = 17$) were penetrated in vivo and showed values of 74 ± 7 mV for membrane potential, 6.94 ± 0.09 pH_i, and 11 ± 5 µM intracellular $\alpha_{CO_3^{2-}}$, from which intracellular $\alpha_{HCO_3^-}$ of 25 ± 10 mM and CO_2 tension of 120 ± 55 Torr were calculated. All ion measurements reached a new steady state in 9 ± 2 s after cell penetration. Thus measurements of intracellular $\alpha_{CO_3^{2-}}$ and pH and associated levels of α_{HCO_3} and CO_2 tension can be determined in biological tissues and cells with a spatial and temporal resolution previously unattainable.

Keywords

bicarbonate; carbonate; pH; carbon dioxide; acid-base; ion-selective microelectrodes

Carbonic acid buffer species play an instrumental role in numerous vital processes of animal cells and tissues. Although CO_2 is often considered a mere waste product, its hydrated and ionized anionic products, HCO_3^- and CO_3^{2-}, are essential for the normal operation of a wide variety of metabolic and physiological processes. For example, HCO_3^- and CO_3^{2-} are physicochemical buffers that, when coupled to membrane-based ion transport systems, create a predominant means of modulating interstitial and intracellular pH (5,8). Furthermore, these same membrane-based ion transport systems and carbonic acid buffer anions are intimately involved in the processes of secretion and absorption (14). Enzymatic reactions that require

carbon moieties as a substrate use HCO_3^- (or CO_3^{2-}) for this purpose (25). Finally, a critical reduction in cellular HCO_3^- stores (as occurs during severe astrocytic acidosis of brain ischemia) is considered to be a potentially important first step toward destruction of neural tissue from a reduction in blood flow (19,21).

Despite these evidences of the widespread biological importance of HCO_3^- and CO_3^{2-}, no means is available to simultaneously monitor all carbonic acid buffer species [i.e., pH, CO_2 tension, and CO_3^{2-} $(\alpha_{CO_3^{2-}})$ and HCO_3^- $(\alpha_{HCO_3^-})$ activities within cells. In this study we show that an anion exchanger, previously reported to be a HCO_3^- sensor (33), is instead highly selective for CO_3^{2-}. This exchanger can be used to measure intracellular $\alpha_{CO_3^{2-}}$ and, when coupled with simultaneous intracellular measurements of pH, can be used to calculate cellular levels of $\alpha_{HCO_3^-}$ and CO_2 tension to a spatial and temporal resolution previously unattainable.

METHODS

Ion-selective microelectrode (ISM) fabrication

The CO_3^{2-} ion exchanger cocktail was prepared from individual components according to Wise (33) and consisted of a 3:1:6 (volume) mixture of tri-*n*-octylpropylammonium chloride (Kodak; Rochester, NY; catalog no. 135 2194, lot no. 809027B), 1-octanol (Fluka, Buchs, Switzerland; catalog no. 74850; lot no. 233468 183) and trifluoroacetyl-*p*-butylbenzene (Specialty Organics, Irwindale, CA; lot no. EG9941). Tri-*n*-octylpropylammonium chloride and 1-octanol were reagent grade and not processed further before use. A gas chromatograph and mass spectrograph of the trifluoroacetyl-*p*-butylbenzene were consistent with analyses previously published for this compound (17) and showed the sample used in this study was 95% pure, with the impurities most likely consisting of *ortho*-and *meta*-isomers of the parent compound. Accordingly, trifluoroacetyl-*p*-butylbenzene was used without further purification.

Single-barrel CO_3^{2-}-sensitive ISMs were fabricated from 1.2-mm OD borosilicate micropipettes (no. 6020 from A-M Systems, Everett, WA) that were silanized with *N,N*-dimethyltrimethylsilylamine (Fluka, Buchs, Switzerland; catalog no. 41720) as previously described (19). ISMs were backfilled with a solution that consisted of (in mM) 23 NaOH, 15 NaCl, 40 NaH$_2$PO$_4$, and 1 NaHCO$_3$ (adjusted to pH 7.1 with HCl). Double-barrel ISMs were also fabricated as previously described (19). The characteristics of the CO_3^{2-} exchanger were determined with ISMs made in either of these two configurations. Triple-barrel ISMs for intracellular use have not previously been reported. Therefore, their fabrication is detailed below.

Triple-barrel borosilicate glass made from 1.2-mm OD tubes (no. 6090 from A-M Systems) was pulled to a tip diameter of ~1 µm. Individual electrode barrels when filled with 0.5 M KC1 had an impedance of 100–150 MΩ. ISM barrels were silanized by a technique modified from Munoz et al. (23). First, the reference barrel was pressurized with N$_2$ gas at 2.7 atmospheres by sealing a thinned 26 gauge Teflon hose carrying the gas into the barrel. Second, the array was mounted vertically in a holder and heated with a hot air gun (200°C). The array was placed immediately in front of the gun's hot air stream and heated for ~1.5 cm of its length, extending back from the tip. Third, a 30 gauge 3-cm-long stainless steel needle connected to N$_2$ gas at 2.7 atmospheres was inserted into the first barrel to be silanized. After 2 min, silanization was begun by altering the pure N$_2$ gas to include *N,N*-dimethyltrimethylsilylamine vapor for 2 min. Silane vapor was removed from the ISM barrel by returning the gas flow back to pure N$_2$ while heating continued for an additional 5 min. Finally, the second ISM barrel was silanized by an analogous procedure. The reference barrel of the silanized array was then filled with 0.5 M

KC1. One ISM barrel was backfilled first with the CO_3^{2-} exchanger and then the CO_3^{2-}-backfill-solution detailed above. The second ISM barrel was converted into a pH-sensitive micropipette by first backfilling it with the tridodecylamine-based pH exchanger, which was followed by phosphate-buffered saline as originally described (2). Arrays were used immediately or stored in 150 mM NaCl for use within 24–48 h.

CO_3^{2-}-sensitive ISM characterization

Activity coefficients for CO_3^{2-} and HCO_3^- were calculated from Debye-Huckel theory using approximate effective ionic radii of these ions in aqueous solutions (see Ref. 11). For example, activity coefficients for CO_3^{2-} and HCO_3^- of Ringer were calculated to be 0.42 and 0.79, respectively, and presumed to be equal to these same values for in vivo measurements. The millivolt response of the CO_3^{2-} ISM was first compared with changes in $\alpha_{HCO_3^-}$ (1, 10, 35, 50, and 100 mM concentration). Fluctuations in test solution pH and $\alpha_{CO_3^{2-}}$ as well as other carbonic acid buffer species were minimized by bubbling the solutions with room air to produce an essentially constant CO_2 tension of 0.1 Torr (32). The relative contribution of changes in $\alpha_{HCO_3^-}$ and $\alpha_{CO_3^{2-}}$ could not be determined by such a "separate solutions" technique (3) because pure solutions of $NaHCO_3$ are never devoid of CO_3^{2-}. This conclusion follows from the mass action equation, which indicates that HCO_3^- will partially ionize to form CO_3^{2-} at a given pH. On the other hand, changes in CO_2 tension within a single $NaHCO_3$ solution induce a relatively immense change in $\alpha_{CO_3^{2-}}$ but only a small change in $\alpha_{HCO_3^-}$ (32). This latter physicochemical fact was used to determine the relative contribution of changes in $\alpha_{CO_3^{2-}}$ to the ISM response in the presence of HCO_3^-. Test solution $\alpha_{CO_3^{2-}}$ was calculated from a known $\alpha_{HCO_3^-}$ and measured pH according to (15,21)

$$\alpha_{CO_3^{2-}} = ([H^+] \times K_2')/\alpha_{HCO_3^-}$$

(1)

where K_2' is the ionization equilibrium constant and equal to 4.68×10^{-11} at 25°C (11).

Anion interference in CO_3^{2-} ISM response was determined by a method similar to that of the "fixed interference" method proposed by Nicholson (24). ISM response to changes in the activity of the principal ion measured (i.e., $\alpha_{CO_3^{2-}}$) in the presence of interfering anions was approximated by an extended Nicolsky-Eisenmann equation (2)

$$mV = B \times \log(\alpha_{CO_3^{2-}} + K_{ij}\alpha_A^{2/z}) + C$$

(2)

where mV is the electrode potential in millivolts, z is the valence of an interfering anion (A), K_{ij} is the equilibrium ratio for association of the j ion with respect to CO_3^{2-}, and B is equal to $nRT/2F$, with R the gas constant (8.2 degree^{-1}·mol^{-1}), T the temperature (°K), F the Faraday constant, and n is an empirical constant chosen so that $nRT/2F$ is the slope of the line when mV are plotted as a function of log $\alpha_{CO_3^{2-}}$ with no interfering anions (i.e., A$^-$) present. If K_{ij} is <1, the ISM has a higher affinity for the principal ion, CO_3^{2-}, than for an interfering anion. Activity coefficients for interfering anions were calculated as above for CO_3^{2-} and HCO_3^- using approximate values for the effective ionic radii of interfering anions (see Ref. 11). The effective

ionic radii for ascorbate, lactate, and glutamate were assumed to be equal to that of acetate (6 Å).

Anion interference was determined by placing the tip of a CO_3^{2-}-ISM in a 10 mM (concentration) $NaHCO_3$ solution with a known concentration of a salt consisting of one anion interferant. Solution pH was continuously monitored. The solution was aerated with room air to induce constant stirring and a relatively stable CO_2 tension and $\alpha_{CO_3^{2-}}$. Once a steady-state pH- and CO_3^{2-}-ISM output were noted, aeration was altered to pure CO_2. When the solution had been maximally acidified, aeration was changed back to room air and periodic (i.e., at least 10 per interferant anion) measurements of pH and CO_3^{2-}-ISM output were recorded as the level of solution acidity returned toward initial conditions. K_{ij} was determined by iteration of linear regression analyses using Eq. 2.

Animal preparation and recording

Rats ($n = 2$) were anesthetized with halothane, a tail artery was cannu-lated, and the animals were placed in a stereotaxic apparatus and artificially ventilated (9,19). Arterial glucose, respiratory gases, and pH were stabilized before intracellular recordings. The left temporalis muscle was exposed and covered with a superfusion cup-pressure foot (19). Triple-barrel ISMs were inserted into temporalis muscle cells through the superfusion cup-pressure foot bathed with warm (35–37°C) Ringer solution. Ringer was gassed with 95% O_2-5% CO_2 (pH 7.35 at 25°C) and contained (in mM) 108 NaCl, 3 KC1, 26 $NaHCO_3$, 1.5 $CaCl_2$, 1.4 $MgCl_2$, 5 glucose, 8 sucrose, and 10 sodium gluconate [modified from Bretag (6)]. The pH within the superfusion cup was periodically monitored with a sem-imicro pH electrode (Microelectrodes, Londonderry, NH; model no. 410). ISMs were connected to two A-1 Axo-probe amplifier systems (Axon Instruments, Burlingame, CA). Reference barrel potentials were electronically subtracted from ion-barrel potentials to yield pure pH and $\alpha_{CO_3^{2-}}$ signals. Data were filtered at 2 Hz and displayed on a strip-chart recorder. A 1 M KCl, 3.5% agar bridge placed on a cervical muscle served as the indifferent electrode. ISM measurements of muscle intracellular pH and $\alpha_{CO_3^{2-}}$ were referenced to their respective values in the superfusate and determined from individual electrode slope responses as described above. Muscle values of $\alpha_{HCO_3^-}$ were calculated from rearrangement of Eq. 1. Intracellular CO_2 tension was calculated from rearrangement of the Henderson-Hasselbalch equation (15,21)

$$CO_2 = \alpha_{HCO_3^-} / S\prime(10^{pH-pK_1'})$$

(3)

where S' is the solubility constant for CO_2 corrected for temperature and equal to 0.0318 at 37°C (29,21) and K_1' is the first ionization constant for carbonic acid corrected for pH and equal to 7.14×10^{-7} at pH 7 and 25°C (21,30,31).

RESULTS

CO_3^{2-}-ISM characteristics

ISMs based on a 3:1:6 (volume) mixture of tri-n-octylpropylammonium chloride, 1-octanol, and trifluoroacetyl-p-butylbenzene responded to changes in $NaHCO_3$ concentration (Fig. 1A). The mV response of a typical ISM is shown. A total of 8–10 measurements were made in each of 5 $NaHCO_3$ solutions (1, 10, 35, 50, and 100 mM concentration). ISM response ($n = 3$) was directly related (correlation coefficient, $r = 0.994$) to the log $\alpha_{HCO_3^-}$. However, this response was not greater than 40.2 mV/decade change in $\alpha_{HCO_3^-}$ (example shown), considerably

less than the 57 mV expected for an ISM that principally sensed a monovalent ionic species (3). This observation, coupled with the fact that pure $NaHCO_3$ solutions contain two anionic species, HCO_3^- and CO_3^{2-}, led to the suspicion that the mV response of these ISMs was measuring some combination of both of these anionic species. Indeed, if the pH of individual $NaHCO_3$ solutions was also measured, an associated $\alpha_{CO_3^{2-}}$ concentration could be calculated and the mV ISM response plotted against changes in this divalent carbonic buffer anion (Fig. 1B). This latter mV response was also highly correlated ($r = 0.990$) to log $\alpha_{CO_3^{2-}}$. Furthermore, the ISM slope response, 23.4 mV, was close to that expected (i.e., 28 mV) for a decade change in principal anionic species measured by an ISM sensitive to divalent ionic species.

Other support for the suggestion that this ISM principally measured CO_3^{2-} anionic species was obtained by varying the CO_2 tension in a pure $NaHCO_3$ solution while simultaneously measuring its pH (Fig. 2). For example, saturating a 10 mM $NaHCO_3$ solution with CO_2 induces an approximate increase of 1% (i.e., μM) in $\alpha_{HCO_3^-}$ but over a 200% decline in $\alpha_{CO_3^{2-}}$. Thus, if the ISM principally measured $\alpha_{HCO_3^-}$, little change in electrode output would have been seen. On the other hand, if the ISM principally sensed $\alpha_{CO_3^{2-}}$, a large mV change in ISM potential should have been seen. Because more than a 50 mV change was observed (Fig. 2), $\alpha_{CO_3^{2-}}$ was the principal carbonic acid buffer anionic species measured by the anionic exchanger cocktail consisting of tri-*n*-octyl-propylammonium chloride, 1-octanol, and trifluoroacetyl-*p*-butylbenzene.

Interference measurements were made three times with three different ISMs for each interfering anion tested as shown in Fig. 2. A mean value interference ratio was calculated. HCO_3^- was always present in test solutions, but its low level of interference meant it did not significantly influence CO_3^{2-} measurements. Concentrations of interfering anions were chosen so as to approximate those found in biological tissues (Table 1). K_{ij} values are given in Table 1 and show that CO_3^{2-}-ISMs are 3,120; 14,667; 385,802; 5,619; 25,895; 282,921; and 359,646 times more sensitive to CO_3^{2-} than to HCO_3^-, chloride, phosphate, ascorbate, lactate glutamate, and acetate ions, respectively, at typical intracellular interferant concentrations expected in biological tissues. No measurable interference was seen for hydroxyl ions. Special mention should be made of how the hydroxyl ion selectivity was determined.

A "fixed" concentration of interferant method (3) could not be used to determine the level of hydroxyl ion interference with CO_3^{2-} measurements. This conclusion stems from the fact that hydroxyl ions and CO_3^{2-} ions simultaneously vary as the pH of a $NaHCO_3$ solution is changed. To overcome this problem we estimated the interference from hydroxyl ions by monitoring CO_3^{2-}-ISM response to large changes in hydroxyl ion concentration in the presence of limited changes in $\alpha_{CO_3^{2-}}$. These conditions were created by monitoring the pH of a 150 mM NaCl solution aerated with room air that has an approximate CO_2 tension of ~0.1 Torr (32). Because the pH and CO_2 tension of the 150 mM NaCl were known, the solution's $\alpha_{HCO_3^-}$ and then $\alpha_{CO_3^{2-}}$ could be determined. Then, after first determining the slope response of a CO_3^{2-}-ISM to changes in $\alpha_{CO_3^{2-}}$ in a $NaHCO_3$ solution (Fig. 2), ISM response was monitored along with pH in a 150 mM NaCl solution. Aliquots of HCl and NaOH were added to adjust pH to 4–8. Within this pH range $\alpha_{CO_3^{2-}}$ was <200 nM. When chloride interference was accounted for, this amount of $\alpha_{CO_3^{2-}}$ was sufficient to account for the 7- to 25-mV change in electrode output noted ($n = 3$) as pH varied from 4 to 8. Thus a measurable hydroxyl interference was unnecessary to account for electrode output.

Muscle intracellular measurements

Skeletal muscle cells were penetrated with triple-barrel ISM arrays made with pH- and CO_3^{2-}-sensitive electrodes to show that carbonic acid buffer species could be dynamically monitored with a temporal and spatial resolution previously unreported. Arterial blood variables in two anesthetized rats were within normal range: O_2 tension: 102 ± 6 Torr; CO_2 tension: 31 ± 1 Torr; pH: 7.46 ± 0.01; systolic blood pressure: 118 ± 2 mmHg; temperature: $37.3 \pm 0.2°C$. Seventeen cells were penetrated and an example of these recordings is shown in Fig. 3. Muscle pH was 6.94 ± 0.09 (range: 6.75–7.05) and membrane potential was 74 ± 7 mV (range: 67–88). Intracellular $\alpha_{CO_3^{2-}}$ was 11 ± 5 µM (range 5–21 µM). Calculated values of $\alpha_{HCO_3^-}$ and CO_2 were 25 ± 10 mM (range: 9–45 mM) and 120 ± 55 Torr (range: 38–357 Torr).

DISCUSSION

The anion exchanger consisting of a 3:1:6 (volume) mixture of tri-*n*-octylpropylammonium chloride, 1-oc-tanol, and trifluoroacetyl-*p*-butylbenzene is highly selective for CO_3^{2-} over other anions typically present in biological tissues (Table 1). Thus this ion exchanger can be used to make accurate measurements of $\alpha_{CO_3^{2-}}$ in interstitial and intracellular space. A commercially available version of this exchanger (WPI, New Haven, CT) was originally tested and found to be selective for CO_3^{2-} (over HCO_3^-) (20). However, this latter exchanger was not felt to be sufficiently selective over other anions to permit useful measurements of $\alpha_{CO_3^{2-}}$ in biological tissues (Ref. 20; R. P. Kraig and S. Rosenfeld, unpublished observations). If these two exchangers are analogous in composition, differences in their anion selectivity may be due to a relative difference in their age. For example, the pH exchanger based on tridodecylamine (2) begins to measure erroneously high levels of intracellular pH in mammalian skeletal muscle cells ~60 days after the pH-sensitive cocktail is mixed (19). Alternatively, selectivity for anion exchangers is primarily determined by ion exchanger solvent, and not ionophore, characteristics (26). Conceivably, selectivity differences between these two ion exchangers could be due to variations between the 1-octanols and trifluoro-*p*-butylbenzenes used. However, since the solvents used in this study are more than 99% and 95% pure, respectively, it is unlikely that unknown impurities account for the observed CO_3^{2-} as opposed to HCO_3^- sensitivity. Further support for this contention comes from the fact that Herman and Rechnitz (17) also used trifluoroacetyl-*p*-butylbenzene as a primary solvent in their CO_3^{2-}-sensitive ion electrode cocktail. Finally, when CO_3^{2-}-sensitive ISMs were backfilled only with 150 mM NaCl, as originally done by Wise (33), their selectivity against HCO_3^- was reduced from that shown in Table 1, and their response to changes in $\alpha_{CO_3^{2-}}$ became supra-Nernstian (data not shown). Yet use of only NaCl as the backfill solution did not diminish ISM response to changes in CO_2 tension of a $NaHCO_3$ solution. Thus backfilling ISMs with 150 mM NaCl did not alter the observation that our anion exchanger mixture predominantly responded to CO_3^{2-} and not HCO_3^-.

Exclusion of the principal ion from backfill solutions alters the Nernstian behavior of ISMs. For example, potassium-sensitive ISMs based on the Corning exchanger 477317 (Corning, Medfield, MA) are nominally sensitive to changes in potassium concentration but also respond to quaternary ammonium compounds (4,12,13). However, response to quaternary ammonium compounds is erratic and produces a non-Nernstian response unless the specific quaternary ammonium compound being measured is included in the backfill solution (12,13). Indeed, when the salt of the quaternary ammonium ion is included in the backfill solution, ISMs made from the 477317 exchanger are strikingly more selective for that quaternary ammonium ion than for potassium (4,12,13). Similar physicochemical phenomena may apply to the anion

exchanger used in this study and help account for its stable and reproducible Nernstian response to CO_3^{2-} as well as its high selectivity for this ion compared with other anions.

Other sensors for carbonic acid buffer species have been reported. However, none of these other sensors has the selectivity, speed or resolution of the triple-barrel CO_3^{2-}- and pH ISM reported here. Another CO_3^{2-} liquid membrane sensor with an apparently high selectivity over HCO_3^- has been reported (17). Notably, trifluoro-*p*-butylbenzene is used as the solvent for this CO_3^{2-} sensor, as it is (along with 1-octanol) for the present CO_3^{2-} sensor. A liquid membrane-based HCO_3^- sensor using a polyvinyl chloride matrix has been reported (16). However, this HCO_3^- sensor has not been miniaturized to an ISM. Furthermore, successful measurements in biological systems with this latter exchanger are likely to be limited, since the exchanger has an extremely slow (i.e., minutes) response time and requires that test solution pH be within a narrow range (16). On the other hand, considerable success has been achieved with use of the CO_2 electrode as designed by Severinghaus and Bradley (28). Combined measurements of tissue CO_2 tension and interstitial pH are possible and can yield meaningful calculations of dynamic changes in interstitial $\alpha_{HCO_3^-}$ changes (20). Unfortunately, such calculations are only an estimate of cellular changes. This conclusion follows from the fact that the CO_2 measurements were made with a CO_2 electrode that had an active surface of square millimeters and thus were only damped averages of actual cellular changes. If a CO_2 electrode is miniaturized to a microelectrode form, its response time rises from a few seconds (20) to several minutes (7). Finally, a combined macro CO_2/pH electrode has been reported (10). However, this device has not been used in biological recordings and has not been miniaturized to a microelectrode form.

Although combined ISM sensors have previously been reported, their fabrication into a device capable of penetrating cells is a rarity. Russell and Brown (27) measured simultaneous intracellular changes in potassium and chloride concentration in snail neurons. Here we show that simultaneous measurements of $\alpha_{CO_3^{2-}}$ and pH are possible. Skeletal muscle intracellular pH (6.94) and membrane potential (74 mV) values, as measured with a triple-barrel ISM, agree well with those previously reported (1,19). Measurements of intracellular $\alpha_{CO_3^{2-}}$ have not been reported. At this time we can only speculate that the wide range (i.e., 5–21 µM) of $\alpha_{CO_3^{2-}}$ measured, and as a result similar magnitude of $\alpha_{HCO_3^-}$ and CO_2 tensions, reflects a true heterogeneity for carbonic acid buffer species within cells. Support for this conjecture comes from calculations that suggest steep gradients within cells between oxygen sources and sinks (18). Similar gradients can be expected for zones of production and consumption of carbonic acid buffer species.

Acknowledgments

REFERENCES

1. Aickin CC, Thomas RC. An investigation of the ionic mechanisms of intracellular pH regulation in mouse soleus muscle fibers. J. Physiol. Lond 1977;273:295–316. [PubMed: 23428]

2. Ammann, D. Ion-Selective Microelectrodes. Berlin: Springer-Verlag; 1981.

3. Ammann D, Lanter L, Steiner RA, Schulthess P, Shijo Y, Simon W. Neutral carrier based hydrogen ion selective microelectrodes for extra- and intracellular studies. Anal. Chem 1981;53:2267–2269. [PubMed: 7316213]

4. Baum G. The influence of hydrophobic interactions on the electrochemical selectivity of liquid membrane response to organic ions. J. Physiol. Chem 1972;76:1872–1875.

5. Boron, WF. Cellular buffering and intracellular pH. In: Seldin, DW.; Giebisch, G., editors. The Regulation of Acid-Base Balance. New York: Raven; 1989. p. 33-56.

6. Bretag AH. Synthetic interstitial fluid for isolated mammalian brain tissue. Life Sci 1969;8:319–329. [PubMed: 5781321]

7. Calfish CR, Carter NW. A micro Pco_2 electrode. Anal. Biochem 1974;60:252–257. [PubMed: 4850223]

8. Chesler M. The regulation and modulation of pH in the nervous system. Prog. Neurobiol 1990;34:401–427. [PubMed: 2192394]

9. Chesler M, KRAIG RP. Intracellular pH transients of mammalian astrocytes. J. Neurosci 1989;9:2011–2019. [PubMed: 2723764]

10. Coon RL, Lai NCJ, Kampine JP. Evaluation of a dual-function pH and Pco_2 in vivo sensor. J. Appl. Physiol 1976;40:625–629. [PubMed: 6422]

11. Dean, JA., editor. Lang's Handbook of Chemistry. 12th ed.. New York: McGraw-Hill; 1979. p. 5-14.

12. Dionne VE. Characterization of drug iontophoresis with a fast microassay technique. Biophys. J 1976;16:705–717. [PubMed: 938714]

13. Dionne VE, Stevens CF. Voltage dependence of agonist effectiveness at the frog neuromuscular junction: resolution of a paradox. J. Physiol. Lond 1975;25:245–270. [PubMed: 1081139]

14. Durham JH, Hardy MA. Bicarbonate, chloride, and proton transport systems. Ann. NY Acad. Sci 1989;574

15. Edsall, JT.; Wyman, J., editors. Biophysical Chemistry. Vol. vol. 1. New York: Academic; 1958.

16. Funck RJJ, Morf WE, Schulthess P, Ammann D, Simon W. Bicarbonate-sensitive liquid membrane electrodes based on neutral carriers for hydrogen ions. Anal. Chem 1982;54:423–429.

17. Herman HB, Rechnitz GA. Preparation and properties of a carbonate ion-selective membrane electrode. Anal. Chim. Acta 1975;76:155–164.

18. Jones DP. Intracellular diffusion gradients of O_2 and ATP. Am. J. Physiol 1986;250:C663–C675. (*Cell Physiol.* 19). [PubMed: 3010727]

19. Kraig RP, Chesler M. Astrocytic acidosis in hyperglycemic and complete ischemia. J. Cereb. Blood Flow Metab 1990;10:104–114. [PubMed: 2298827]

20. Kraig RP, Cooper AJL. Bicarbonate and ammonia changes in brain during spreading depression. Can. J. Physiol. Pharmacol 1987;65:1099–1104. [PubMed: 3621035]

21. Kraig RP, Pulsinelli WA, Plum F. Carbonic acid buffer changes during complete brain ischemia. Am. J. Physiol 1986;250:R348–R357. (*Regulatory Integrative Comp. Physiol.* 19). [PubMed: 3082219]

22. McIlwain, H.; Bachelard, HS. Biochemistry and the Central Nervous System. New York: Churchill-Livingston; 1971.

23. Munoz JL, Deyhimi F, Coles JA. Silanization of glass in the making of ion-selective microelectrodes. J. Neurosci. Methods 1983;8:231–247. [PubMed: 6312200]

24. Nicholson C, ten Bruggencate G, Stockle H, Steinberg R. Calcium and potassium changes in extracellular mi-croenvironment of cat cerebellar cortex. J. Neurophysiol 1978;41:1026–1039. [PubMed: 681986]

25. Patel MS. The relative significance of CO_2-fixing enzymes in the metabolism of rat brain. J. Neurochem 1974;22:717–724. [PubMed: 4152139]

26. Reinsfelder RE, Schultz FA. Anion selectivity studies on liquid membrane electrodes. Anal. Chim. Acta 1973;65:425–435.

27. Russell JM, Brown AM. Active transport of potassium and chloride in an identifiable *Molluscan* neuron. Science Wash. DC 1972;175:1475–1477.

28. Severinghaus JW, Bradley AF. Electrodes for blood Po_2 and Pco_2 determination. J. Appl. Physiol 1957;13:515–520. [PubMed: 13587443]

29. Slesjo BK. The solubility of carbon dioxide in cerebral cortical tissue from rat at 37.5°C. With a note on the solubility of carbon dioxide in 0.16 M NaCl and cerebrospinal fluid. Acta Physiol. Scand 1962;55:325–341. [PubMed: 13912691]

30. Siesjo BK. The bicarbonate/carbonic acid buffer system of the cerebral cortex of cats, as studied in tissue homogenates. II. The pK_1 of carbonic acid at 37.5°C, and the relation between carbon dioxide tension and pH. Acta Neurol. Scand 1962;38:121–141. [PubMed: 13912690]

31. Siggaard, Andersen, O. The first dissociation exponent of carbonic acid as a function of pH. Scand. J. Clin. Lab. Invest 1962;14:587–597. [PubMed: 14012797]

32. Stewart, PA. How to Understand Acid-Base. New York: Elsevier; 1981.

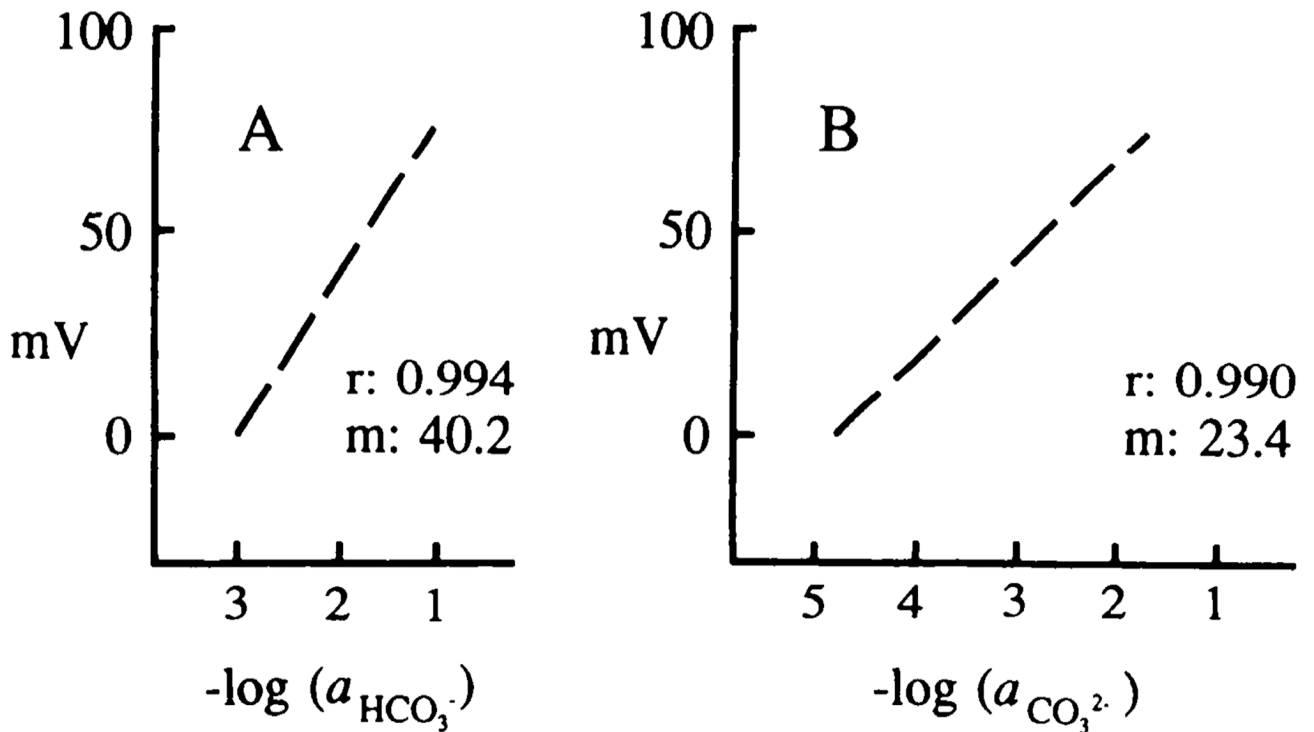33. Wise, WM., inventor. Bicarbonate Ion-Sensitive Electrode. U. S. Patent. 3,723,281. 1973.

FIG. 1.

Response of CO_3^{2-}-sensitive ISM to changes in carbonic acid anion concentration. *A*: ISM response in millivolts (mV) was directly related (correlation coefficient, $r = 0.994$) to changes in the logarithm of $\alpha_{HCO_3^-}$ (1, 10, 35, 50, and 100 mM). The standard deviation of 5 measurements made at each concentration was less than the diameter of the dashed line. Accordingly, individual data points are not shown. Electrode slope (*m*) (i.e., mV/decade changes in $\alpha_{HCO_3^-}$) was ($n = 3$) not greater than 40.2 mV (example shown) and considerably less than the 57 mV expected for an ISM that sensed monovalent anions at room temperature. On the other hand, when ISM output was compared with the corresponding logarithm of $\alpha_{CO_3^{2-}}$, associated with the above $\alpha_{HCO_3^-}$, a highly linear relationship ($r = 0.990$) was noted with a slope of 23.4 mV/ decade change in $\alpha_{CO_3^{2-}}$, near the ideal value of 28.5 mV predicted for an ISM that responded to divalent ions (*B*). The linearity of ISM output compared with concentration change suggests that little ionic interference with the principal ion measured was seen. However, whether the ISM principally measures HCO_3^- or CO_3^{2-} cannot be determined by simply comparing ISM output to concentration changes.
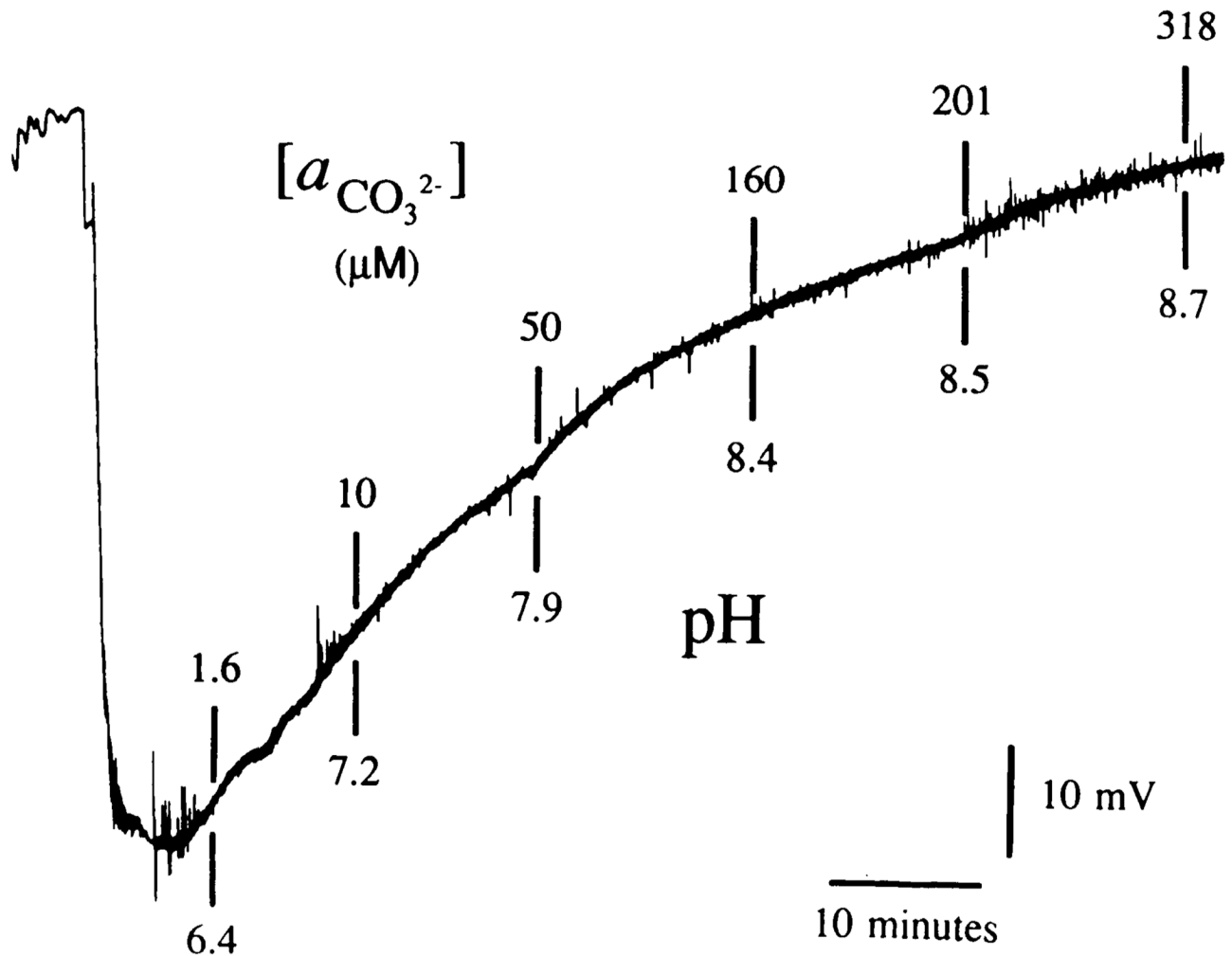
$$[a_{CO_3^{2-}}]$$

(μM)

318

201

160

50

10

1.6

8.7

8.5

8.4

7.9

7.2

6.4

pH

10 mV

10 minutes

FIG. 2.

Potential response of a CO_3^{2-}-sensitive ISM to changes in CO_2 tension in $NaHCO_3$. Record shown is the millivolt (mV) response of an ISM to changes in CO_2 within a 10 mM (concentration) solution of $NaHCO_3$. Such an alteration in gas tension will cause a small (i.e., μM) increase in $\alpha_{HCO_3^-}$ but more than a 200% increase in $\alpha_{CO_3^{2-}}$. This simple, physicochemical fact can be used to determine if the ISM principally measures $\alpha_{HCO_3^-}$ or $\alpha_{CO_3^{2-}}$ in a $NaHCO_3$ solution. Here a 10 mM $NaHCO_3$ solution was initially aerated with N_2 (*top left*). Exposure to CO_2 caused a prompt fall in solution pH to <6.4 (*bottom left*). At the same time ISM potential dropped by more than 50 mV, indicating that the ISM primarily measured $\alpha_{CO_3^{2-}}$ and not $\alpha_{HCO_3^-}$. Finally, solution aeration was changed back to N_2 (lower left of chart record). As solution CO_2 tension dropped from this latter maneuver pH rose from <6.4 to >8.7 (as noted by specific solution pH measurements indicated below vertical lines). $\alpha_{CO_3^{2-}}$ is shown above vertical lines.
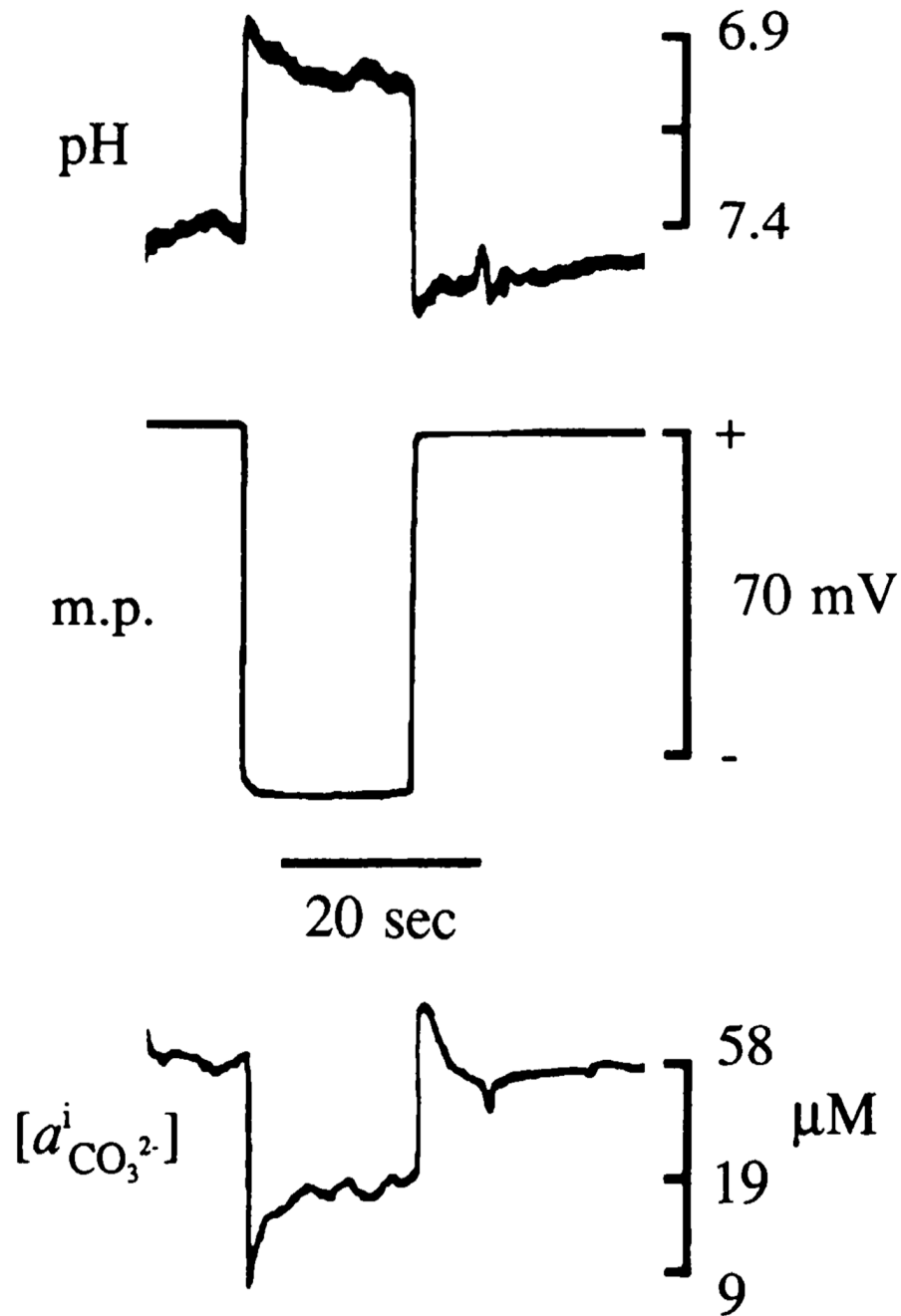
FIG. 3.

Intracellular record from skeletal muscle cell penetration with a triple-barrel ISM array consisting of pH-, CO_3^{2-}-, and potential-sensing electrodes. Skeletal muscle cells in a temporalis muscle of an anesthetized and artificially ventilated rat were penetrated with a triple-barrel ISM array. *Top*: change in pH from interstitial level of 7.4 to that typically seen in skeletal muscle cells of 7.0 as array penetrates a cell. *Middle*: simultaneous measurement of membrane potential that in this instance exceeds 70 mV. *Bottom*: measured change in $\alpha_{CO_3^{2-}}$ as array moves from interstitial to intracellular space. CO_3^{2-} and pH measurements reached a new steady state <9 s after muscle cell penetration.

TABLE 1

CO_3^{2-}-ion-selective micropipette selectiuities

Anion	Intracellular Concentration, M	Selectivity Constant	Relative Selectivity
Chloride[*]	0.010	6.8×10^{-5}	3,120:1
Bicarbonate[†]	0.018	1.2×10^{-9}	14,667:1
Di- and monohydrogen phosphate[*]	0.001	5.5×10^{-5}	385,862:1
Ascorbate[‡]	0.0008	5.9×10^{-3}	5,619:1
Lactate[‡]	0.001	5.9×10^{-7}	25,895:1
Glutamate[‡]	0.010	7.5×10^{-10}	282,921:1
Acetate[‡]	0.001	5.9×10^{-8}	359,646:1
Hydroxyl	10^{-7}		

[*] Taken from Ref. [32];

[†] calculated from muscle measurements made in this study;

[‡] taken from Ref. [22]. Missing values were estimated as too small to measure since electrode output could be accounted for without inclusion of an interference term for hydroxyl ions.